

RAPID COMMUNICATIONS

The purpose of this Rapid Communications section is to provide accelerated publication of important new results in the fields regularly covered by Journal of Materials Research. Rapid Communications cannot exceed four printed pages in length, including space allowed for title, figures, tables, references, and an abstract limited to about 100 words.

(Fe,Co,Ni)-B-Si-Nb bulk glassy alloy with super-high strength and some ductility

Baolong Shen^{a)} and Akihisa Inoue

Institute for Materials Research, Tohoku University, Sendai 980-8577, Japan; and Research and Development Project, Core Research for Evolution Science and Technology (CREST), Japan Science and Technology Agency, Sendai 980-8577, Japan

(Received 8 May 2004; accepted 3 September 2004)

Glassy [(Fe_{0.8}Co_{0.1}Ni_{0.1})_{0.75}B_{0.2}Si_{0.05}]₉₆Nb₄ alloy rods with glass transition temperature of 835 K, followed by a large supercooled liquid region of 55 K were produced in the diameter range up to 2 mm by copper mold casting. The glassy alloy rods exhibit super-high true fracture strength of 4225 MPa combined with elastic strain of 0.02 and true plastic strain of 0.005. The super-high strength alloy simultaneously exhibits high magnetization of 1.1 T, low coercivity of 3 A/m, and high permeability of 1.8×10^4 at 1 kHz. The success of synthesizing a super-high strength Fe-based bulk glassy alloy with some compressive plastic strain and good soft magnetic properties is encouraging for future development of Fe-based bulk glassy alloys as new engineering and functional materials.

Since the first syntheses of bulk glassy alloys in lanthanide (Ln)- and Mg-based systems by copper mold casting in 1989,^{1,2} a large number of bulk glassy alloys have been developed, and some glassy alloys have been used as practical materials.³ Although the formation of bulk glassy alloys before 1995 was limited to a nonferrous alloy system,³ an Fe-based bulk glassy alloy was synthesized for the first time in an Fe-(Al,Ga)-metalloid system in 1995.⁴ Subsequently, a variety of Fe- and Co-based bulk glassy alloy systems have been synthesized.⁵⁻⁹ However, these reports concentrated on the subject of magnetic properties because of potential magnetic applications. Considering that the mechanical properties of Fe- and Co-based bulk glassy alloys are also very important for their applications as structural materials, we have investigated the mechanical properties of the Fe- and Co-based bulk glassy alloys and found that the Co-Fe-Ta-B bulk glassy alloy exhibits ultrahigh strength above 5000 MPa and very high Young's modulus of 268 GPa.¹⁰ For the Fe-based bulk glassy alloys, it was also found that the (Fe_{0.75}B_{0.15}Si_{0.1})₉₆Nb₄ and Fe₇₇Ga₃P_{9.5}C₄B₄Si_{2.5} bulk glassy alloys exhibit high

strength of 3000 MPa.¹¹ Recently, several new Fe-based bulk glassy alloy systems with fracture strengths of 3000–4000 MPa in the absence of casting-induced defects were developed by the Poon and Liu groups.¹²⁻¹⁵ This communication reports the synthesis, structures, and mechanical properties of [(Fe_{0.8}Co_{0.1}Ni_{0.1})_{0.75}B_{0.2}Si_{0.05}]₉₆Nb₄ bulk glassy alloy with record super-high strength over 4000 MPa for the Fe-based bulk alloys.

Multi-component Fe-based alloy ingots with compositions of [(Fe_{1-x-y}Co_xNi_y)_{0.75}B_{0.25-z}Si_z]₉₆Nb₄ were prepared by arc melting the mixtures of pure Fe, Co, Ni, and Nb metals, and pure B and Si crystals in an argon atmosphere. The alloy compositions represent nominal atomic percentages. Cylindrical alloy rods with a length of 50 mm and different diameters of 1–3 mm were produced by the copper mold casting method. Glassy and crystallized structures were examined by x-ray diffraction (XRD) with Cu K α radiation and high-resolution transmission electron microscopy (HRTEM). Cylindrical alloy rods in as-cast and annealed states were sectioned by fine cutter for XRD measurement. To anneal the samples, the rods were first placed in fused silica tubes that were sealed after evacuation. Then the fused silica tubes were put into the furnace, and the samples were heated rapidly and then quenched in water. Thermal stability associated with glass transition temperature (T_g), crystallization

^{a)}Address all correspondence to this author.

e-mail: shen@imr.tohoku.ac.jp

DOI: 10.1557/JMR.2005.0001

temperature (T_x), and supercooled liquid region ($\Delta T_x = T_x - T_g$) was examined by differential scanning calorimetry (DSC) at a constant heating rate of 0.67 K/s. The liquidus temperature (T_l) of the alloy was examined by differential thermal analysis (DTA). Mechanical properties including Young's modulus (E), compressive true yield ($\sigma_{c,y}$) and fracture ($\sigma_{c,f}$) strength, and compressive true elastic ($\epsilon_{c,e}$) and plastic ($\epsilon_{c,p}$) strain were measured with an Instron 4204 (Instron Corporation, Canton, MA) testing machine. The gauge dimensions were 2-mm diameter and 4-mm length, and the strain rate was $5.0 \times 10^{-4} \text{ s}^{-1}$. Vickers hardness was measured with a Vickers hardness tester under a load of 1.96 N. Deformation and fracture behaviors were examined by scanning electron microscopy (SEM). Magnetic properties of saturation magnetization (I_s), coercive force (H_c), and effective permeability at 1 kHz (μ_e) were measured with a vibrating sample magnetometer (VSM) under an applied field of 400 kA/m, a B-H loop tracer under a field of 800 A/m, and an impedance analyzer under a field of 1 A/m, respectively. Curie temperature (T_c) was determined from the DSC curve.

Figure 1 shows DSC curves of the $[(\text{Fe}_{0.8}\text{Co}_{0.1}\text{Ni}_{0.1})_{0.75}\text{B}_{0.2}\text{Si}_{0.05}]_{96}\text{Nb}_4$ glassy alloy rods with diameters of 1.5 and 2 mm, together with the data of

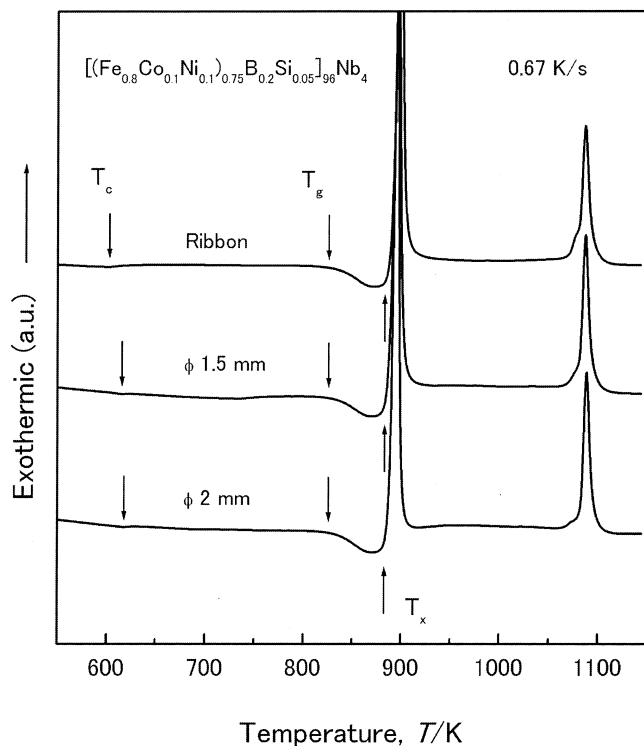


FIG. 1. Differential scanning calorimetry curves of bulk glassy $[(\text{Fe}_{0.8}\text{Co}_{0.1}\text{Ni}_{0.1})_{0.75}\text{B}_{0.2}\text{Si}_{0.05}]_{96}\text{Nb}_4$ alloy rods with diameters of 1.5 and 2 mm. The data of the melt-spun glassy alloy ribbon are also shown for comparison.

the melt-spun glassy alloy ribbon. The bulk alloys exhibited distinct glass transition at 835 K, followed by a large supercooled liquid region of 55 K. No appreciable difference in T_g , T_x , ΔT_x , and crystallization process is observed between the melt-spun ribbon and rod samples, though Curie temperature (T_c) increases with an increase of diameter. The increase of T_c is interpreted to result from the progress of structural relaxation as the diameter of the glassy alloy rod increases.¹⁶ Besides, the crystallization occurs through two exothermic peaks.

Figure 2 shows XRD patterns of the $[(\text{Fe}_{0.8}\text{Co}_{0.1}\text{Ni}_{0.1})_{0.75}\text{B}_{0.2}\text{Si}_{0.05}]_{96}\text{Nb}_4$ glassy alloy subjected to annealing for 60 s at temperatures of 853 and 868 K, and for 600 s at 943 and 1133 K, corresponding to the temperatures just above the first and the second exothermic peaks, respectively. The XRD pattern of the as-cast bulk alloy is also shown for comparison. The as-cast alloy has a glassy structure, and its structure remains almost unchanged

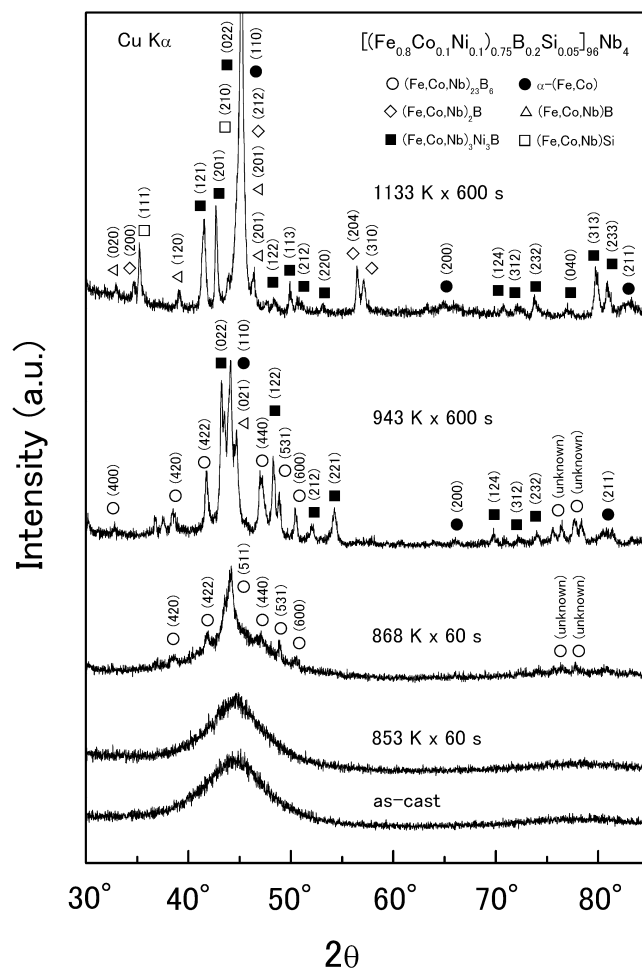


FIG. 2. XRD patterns of $[(\text{Fe}_{0.8}\text{Co}_{0.1}\text{Ni}_{0.1})_{0.75}\text{B}_{0.2}\text{Si}_{0.05}]_{96}\text{Nb}_4$ glassy alloy samples annealed for 60 s at 853 and 868, and for 600 s at 943 and 1133 K. The pattern of the as-cast bulk alloy is also shown for comparison.

even after annealing at 853 K. The XRD patterns for the sample annealed at 868 K are identified as a single phase of face-centered cubic Fe_{23}B_6 type structure with a large lattice parameter of more than 1 nm and in which Co and Nb dissolved.¹⁷ The precipitations for the sample annealed at 943 K corresponding to the temperature above the first exothermic peak are a mixture of $(\text{Fe,Co,Nb})_{23}\text{B}_6$, $(\text{Fe,Co,Nb})_3\text{Ni}_3\text{B}$, and $\alpha\text{-(Fe,Co)}$ phases. We also confirmed that the structure after annealing for 600 s at 1133 K corresponding to the second exothermic peak consisted of $\alpha\text{-(Fe,Co)}$, $(\text{Fe,Co,Nb})\text{B}$, $(\text{Fe,Co,Nb})_2\text{B}$, $(\text{Fe,Co,Nb})_3\text{Ni}_3\text{B}$, and $(\text{Fe,Co,Nb})\text{Si}$ phases. Therefore, it is concluded that the primary precipitation phase of the $(\text{Fe,Co,Nb})_{23}\text{B}_6$ is in a metastable state. It has been pointed out by Imafuku et al. that the essential structural feature in Fe–Nb–B glassy alloys is the distorted dense random network of trigonal prisms connected with each other through glue atoms of Nb, which leads to the high stability of supercooled liquid against crystallization.^{18,19} On the other hand, crystallization of the $(\text{Fe,Co,Nb})_{23}\text{B}_6$ phase from the networklike structure requires long-range atomic rearrangements of constituent elements, which also improves the thermal stability of supercooled liquid, and therefore enables the formation of a larger bulk glassy alloy by the copper mold casting process.²⁰

Figure 3 shows the compressive true stress-strain curve of the $[(\text{Fe}_{0.8}\text{Co}_{0.1}\text{Ni}_{0.1})_{0.75}\text{B}_{0.2}\text{Si}_{0.05}]_{96}\text{Nb}_4$ glassy alloy rod. As shown in the curve, the glassy alloy exhibits $\epsilon_{c,e}$ up to 0.02, followed by $\epsilon_{c,p}$ of 0.005 and then final fracture. E and $\sigma_{c,f}$ are as high as 208 GPa and

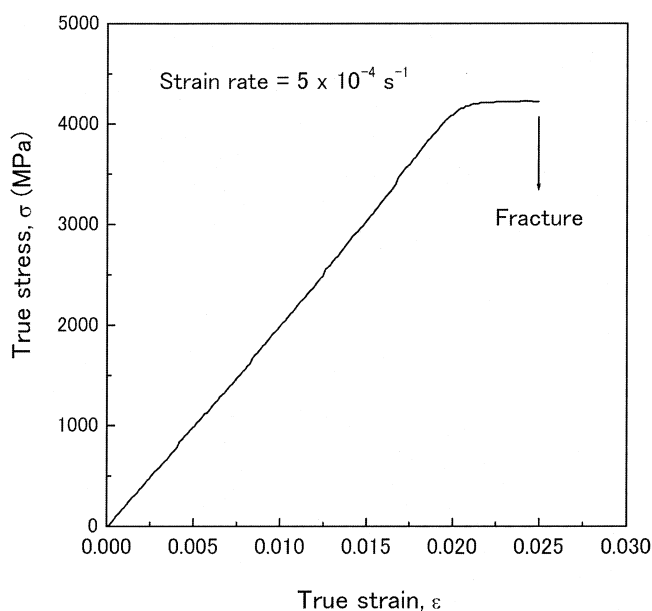


FIG. 3. Compressive true stress-strain curve of bulk glassy $[(\text{Fe}_{0.8}\text{Co}_{0.1}\text{Ni}_{0.1})_{0.75}\text{B}_{0.2}\text{Si}_{0.05}]_{96}\text{Nb}_4$ alloy rod with a diameter of 2 mm.

4225 MPa, respectively, and $\sigma_{c,y}$ is defined by the deviation from the linear relation in true stress–strain curve is 4150 MPa. The mechanical behavior of the glassy alloy is approximately elastic–perfectly plastic. One of the reasons for the super-high strength is interpreted to result from strong bonding nature between the transition metals and metalloids. It has been pointed out by Chen et al. that electrons transfer from the metalloids, fill the d shells of transition metals, and then s – d hybrid bonding is formed.^{21,22} In this study, it is presumed that the s – d hybrid bonding would become stronger by adding Co and Ni transition metal as well as increasing B content. The s – d hybrid bonding would hinder the interparticle displacements and, therefore, raise the elastic modulus. One of the other reasons for the super-high strength is attributed to the mixing enthalpies with large negative values. The enthalpy of mixing is -9 kJ/mol for the Co–B pair, -21 kJ/mol for the Co–Si pair, -25 kJ/mol for the Co–Nb pair, -9 kJ/mol for the Ni–B pair, -23 kJ/mol for the Ni–Si pair, -30 kJ/mol for the Ni–Nb pair, -11 kJ/mol for the Fe–B pair, -18 kJ/mol for Fe–Si pair, -16 kJ/mol for the Fe–Nb pair, and -39 kJ/mol for the B–Nb pair.²³ It can be seen that the mixing enthalpies with negative values of the atomic pairs between Co and Si or Nb, Ni and Si or B are larger than those of the atomic pairs between Fe and Si or Nb, and the mixing

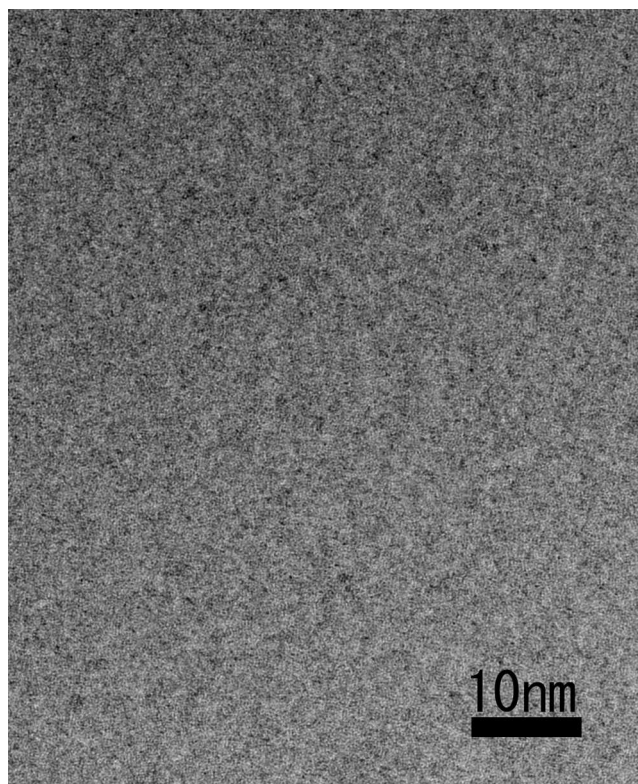


FIG. 4. High-resolution TEM image of bulk glassy $[(\text{Fe}_{0.8}\text{Co}_{0.1}\text{Ni}_{0.1})_{0.75}\text{B}_{0.2}\text{Si}_{0.05}]_{96}\text{Nb}_4$ alloy rod with a diameter of 2 mm.

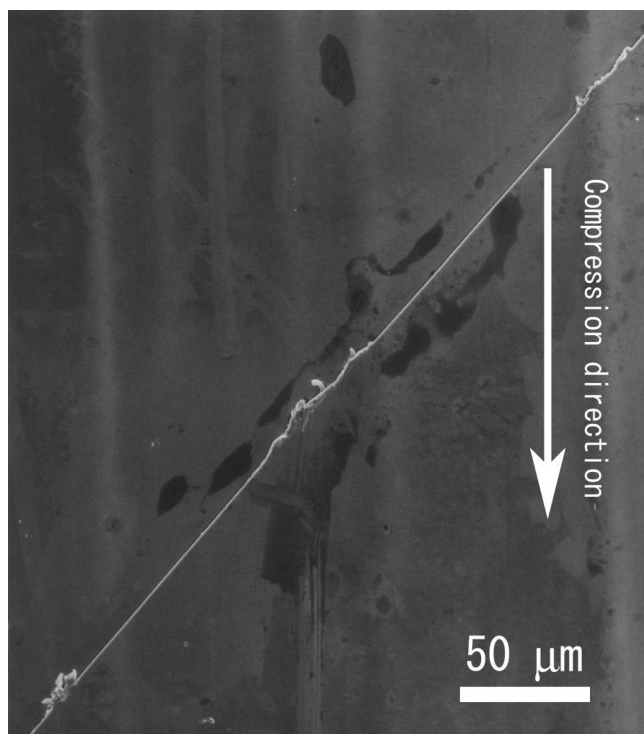


FIG. 5. Scanning electron micrograph (SEM) image of outer lateral surface of the bulk glassy $[(\text{Fe}_{0.8}\text{Co}_{0.1}\text{Ni}_{0.1})_{0.75}\text{B}_{0.2}\text{Si}_{0.05}]_{96}\text{Nb}_4$ alloy rod subjected to the strain of 0.0225 but unloaded before fracture.

enthalpy with negative values for the B–Nb atomic pair is as large as 39 kJ/mol. Therefore, it can be also considered that the super-high fracture strength of the present Fe-based bulk glassy alloy system is resulted from the addition of Co and Ni as well as the increase of B content. In addition, when Co and Ni elements are added and the B content increases, the ΔT_x increases to 55 K, but a reduced glass transition temperature (T_g/T_1) is maintained at 0.61 (compare with previous results of Fe–B–Si–Nb bulk glassy alloy).²⁴ This enabled us to successfully prepare Fe-based bulk glassy alloy rods with diameters up to 2 mm.

After final failure, the fracture surface consisted of vein and smooth patterns typical to glassy alloys with ductility. Figure 4 shows a HRTEM image of the $[(\text{Fe}_{0.8}\text{Co}_{0.1}\text{Ni}_{0.1})_{0.75}\text{B}_{0.2}\text{Si}_{0.05}]_{96}\text{Nb}_4$ glassy alloy rod with a diameter of 2 mm. Only modulated contrast typical to a glassy single structure is observed. It is therefore concluded that the super-high strength of the Fe-based bulk glassy alloy originates from the glassy structure.

Figure 5 shows SEM images revealing deformation behavior of the alloy rod with the $\sigma_{c,f}$ of 4225 MPa subjected to the strain of 0.0225 but unloaded before fracture. Only a localized main shear band can be observed on the surface of the rod as shown in the figure, and its angle with stress axis is measured to be 43° , which is in agreement with the other results.²⁵ It needs to emphasize that this is the first time of obtaining such a

result for Fe-based bulk glassy alloy because of the difficulties of preparing and testing Fe-based bulk glassy alloy up to date. Besides, we cannot find any cracks on the lateral surface of the rod which was strained up to 0.0225. Therefore, it is proposed that the plastic deformation is responsible for the addition of Ni element though mechanism remains unclear.

In summary, a new Fe-based bulk glassy alloy $[(\text{Fe}_{0.8}\text{Co}_{0.1}\text{Ni}_{0.1})_{0.75}\text{B}_{0.2}\text{Si}_{0.05}]_{96}\text{Nb}_4$ with high glass-forming ability, super-high fracture strength, and distinct plasticity was successfully synthesized. Additionally, the super-high strength alloy simultaneously exhibits high magnetization of 1.1 T, low coercivity of 3 A/m, and high permeability of 1.8×10^4 at 1 kHz. These excellent properties allow us to expect that the new Fe-based bulk glassy alloy will be used as a new engineering and functional material on parts of micromotors, radio wave clock antennas, watch gears, and other applications.

REFERENCES

1. A. Inoue, K. Ohtera, K. Kita, and T. Masumoto: New amorphous Mg–Ce–Ni alloys with high strength and good ductility. *Jpn. J. Appl. Phys.* **27**, L2248 (1988).
2. A. Inoue, T. Zhang, and T. Mosumoto: Al–La–Ni amorphous alloys with a wide supercooled liquid region. *Mater. Trans. JIM* **30**, 965 (1989).
3. A. Inoue: Stabilization of metallic supercooled liquid and bulk amorphous alloys. *Acta Mater.* **48**, 279 (2000).
4. A. Inoue, Y. Shinohara, and J.S. Gook: Thermal and magnetic properties of bulk Fe-based glassy alloys prepared by copper mold casting. *Mater. Trans. JIM* **36**, 1427 (1995).
5. T.D. Shen and R.B. Schwarz: Bulk ferromagnetic glasses prepared by flux melting and water quenching. *Appl. Phys. Lett.* **75**, 49 (1999).
6. J.M. Borrego, A. Conde, S. Roth, and J. Eckert: Glass-forming ability and soft magnetic properties of FeCoSiAlGaPCB amorphous alloys. *J. Appl. Phys.* **92**, 2073 (2002).
7. P. Pawlik, H.A. Davies, and M.R.J. Gibbs: Magnetic properties and glass formability of $\text{Fe}_{61}\text{Co}_{10}\text{Zr}_5\text{W}_4\text{B}_{20}$ bulk metallic glassy alloy. *Appl. Phys. Lett.* **83**, 2775 (2003).
8. B.L. Shen, H. Koshiba, A. Inoue, H.M. Kimura, and T. Mizushima: Bulk glassy $\text{Co}_{43}\text{Fe}_{20}\text{Ta}_{5.5}\text{B}_{31.5}$ alloy with high glass-forming ability and good soft magnetic properties. *Mater. Trans.* **42**, 2136 (2001).
9. H. Chiriac, N. Lupu, and M. Tibu: Design and preparation of new Fe-based bulk amorphous alloys torroids. *IEEE Trans. Magn.* **39**, 3040 (2003).
10. A. Inoue, B.L. Shen, H. Koshiba, H. Kato, and A.R. Yavari: Cobalt-based bulk glassy alloy with ultrahigh strength and soft magnetic properties. *Nat. Mater.* **2**, 661 (2003).
11. A. Inoue, B.L. Shen, A.R. Yavari, and A.L. Greer: Mechanical properties of Fe-based bulk glassy alloys in Fe–B–Si–Nb and Fe–Ga–P–C–B–Si systems. *J. Mater. Res.* **18**, 1487 (2003).
12. V. Ponnambalam, S.J. Poon, G.J. Shiflet, V.M. Keppens, R. Taylor, and G. Petculescu: Synthesis of iron-based bulk metallic glasses as nonferromagnetic amorphous steel alloys. *Appl. Phys. Lett.* **83**, 1131 (2003).
13. V. Ponnambalam, S.J. Poon, and G.J. Shiflet: Fe-based bulk metallic glasses with diameter thickness larger than one centimeter. *J. Mater. Res.* **19**, 1320 (2004).

14. Z.P. Lu, C.T. Liu, and W.D. Porter: Role of yttrium in glass formation of Fe-based bulk metallic glasses. *Appl. Phys. Lett.* **83**, 2581 (2003).
15. Z.P. Lu, C.T. Liu, J.R. Thompson, and W.D. Porter: Structural amorphous steels. *Phys. Rev. Lett.* **92**, 245503 (2004).
16. H.S. Chen: Glassy metals. *Rep. Prog. Phys.* **43**, 353 (1980).
17. M. Imafuku, S. Sato, H. Koshiba, E. Matsubara, and A. Inoue: Structural variation of Fe-Nb-B metallic glasses during crystallization process. *Scripta Mater.* **44**, 2369 (2001).
18. M. Imafuku, S. Sato, H. Koshiba, E. Matsubara, and A. Inoue: Crystallization behavior of amorphous $\text{Fe}_{90-x}\text{Nb}_{10}\text{B}_x$ ($X = 10$ and 30) alloys. *Mater. Trans. JIM* **41**, 1526 (2000).
19. M. Imafuku, S. Sato, E. Matsumara, and A. Inoue: Structural study of $\text{Fe}_{90-x}\text{Nb}_{10}\text{B}_x$ ($x = 10, 20$ and 30) glassy alloys. *J. Non-Cryst. Solids* **312**, 589 (2002).
20. E. Matsubara, S. Sato, M. Imafuku, T. Nakamura, H. Koshiba, A. Inoue, and Y. Waseda: Structural study of amorphous $\text{Fe}_{10}\text{M}_{10}\text{B}_{20}$ ($M = \text{Zr, Nb, and Cr}$) alloys by x-ray diffraction. *Mater. Sci. Eng. A* **312**, 136 (2001).
21. H.S. Chen, J.T. Krause, and E. Coleman: Elastic constants, hardness and their implications to flow properties of metallic glasses. *J. Non-Cryst. Solids* **18**, 157 (1975).
22. H.S. Chen: Correlation between elastic constants and flow behavior in metallic glasses. *J. Appl. Phys.* **49**, 462 (1978).
23. F.R. De Boer, R. Boom, W.C.M. Mattens, A.R. Miedema, and A.K. Niessen: Experimental and predicted enthalpies of alloy formation, in *Cohesion in Metals*, edited by F.R. de Boer and D.G. Pettifor (North-Holland, Amsterdam, The Netherlands, 1989), pp. 217–258.
24. A. Inoue and B.L. Shen: Soft magnetic bulk glassy Fe-B-Si-Nb alloys with high saturation magnetization above 1.5 T. *Mater. Trans.* **43**, 766 (2002).
25. Z.F. Zhang, J. Eckert, and L. Schultz: Difference in compressive and tensile fracture mechanisms of $\text{Zr}_{59}\text{Cu}_{20}\text{Al}_{10}\text{Ni}_8\text{Ti}_3$ bulk metallic glass. *Acta Mater.* **51**, 1167 (2003).